



HAL
open science

Natural hydraulic lime for blended cement mortars: Behavior from fresh to hardened states

R. Jaafri, Abdelilah Aboulayt, S.Y. Alam, Emmanuel Rozière, Ahmed Loukili

► To cite this version:

R. Jaafri, Abdelilah Aboulayt, S.Y. Alam, Emmanuel Rozière, Ahmed Loukili. Natural hydraulic lime for blended cement mortars: Behavior from fresh to hardened states. *Cement and Concrete Research*, 2019, 120, pp.52 - 65. 10.1016/j.cemconres.2019.03.003 . hal-03484794

HAL Id: hal-03484794

<https://hal.science/hal-03484794>

Submitted on 20 Dec 2021

HAL is a multi-disciplinary open access archive for the deposit and dissemination of scientific research documents, whether they are published or not. The documents may come from teaching and research institutions in France or abroad, or from public or private research centers.

L'archive ouverte pluridisciplinaire **HAL**, est destinée au dépôt et à la diffusion de documents scientifiques de niveau recherche, publiés ou non, émanant des établissements d'enseignement et de recherche français ou étrangers, des laboratoires publics ou privés.



Distributed under a Creative Commons Attribution - NonCommercial 4.0 International License

Natural hydraulic lime for blended cement mortars: Behavior from fresh to hardened states

R. JAAFRI¹, A. ABOULAYT¹, S.Y. ALAM¹, E. ROZIERE¹, A. LOUKILI¹

¹ Ecole Centrale de Nantes, Institut de Recherche en Génie Civil et Mécanique (GeM), UMR-CNRS 6183, 1 rue de la Noë, BP 92101, F-44321 Nantes, France

Abstract

This paper presents the influence of natural hydraulic lime (NHL) on the behavior of cement-based materials at fresh and hardened states. Two reference mortars with and without limestone filler (LF) and with water-to-cement ratio of 0.6 were considered. For each reference mixture, cement was replaced by NHL with increasing mass proportions of 12.5%, 25% and 50%, while maintaining a constant paste volume. The freshly mixed **pastes and mortars** were tested for rheology, hydration process and setting properties. Moreover, plastic and drying shrinkage and compressive strength were also measured. The methodology shows that the substitution of cement by NHL affects the rheological behavior and the compressive strength, but improves the homogeneity of the mixtures. The incorporation of NHL also generated an expansion period resulting in a significant decrease in plastic shrinkage, and mitigated long-term drying shrinkage. The effects of substitution of cement by NHL during fresh and hardened states are presented along with the analysis of underlying mechanisms. The findings of this paper highlight the benefits of using NHL to optimize mortars' mix-design in terms of workability, mechanical properties and delayed behavior.

Key words:

Natural hydraulic lime, hydration, plastic shrinkage, mineral addition, drying shrinkage

1. Introduction

Floor screed is part of the finishing work that takes place once the structural work is completed. Fluid screeds made of calcium sulphate have been available in the market for nearly 20 years and self-leveling cementitious screeds for nearly 10 years. Recently their market share has gone up sharply due to their beneficial technical features and ease of implementation. The cement-based screeds are often used as they do not show sensitivity to moisture and enable faster setting.

Fluid screeds are very easy to implement and offer many advantages, such as low thickness and rapid hardening. The mix-design of self-leveling screeds is a compromise between fluidity which ensures easy implementation and the required consistency to avoid phase separation problems, including segregation and bleeding [1]. It is usually considered that the mixture is a concentrate suspension in which the viscous and dense phase is the paste (powders ($<125\mu\text{m}$) + water + mineral or chemical admixtures), and the less concentrated dispersed phase is based on the coarser particles (sand). It is actually necessary to limit the sand content and to maintain a sufficient paste volume in order to limit the inter-granular contacts and the risk of blocking; the fluidity of the whole mixture is closely related to the amount and fluidity of the paste [1].

The use of mineral additions as cement replacement is a common practice to limit the cement content induced by increasing the paste volume. The limestone fillers are among the most widely used additions, and this is due to their large local availability and their moderate price. Furthermore, the formulation of a fluid cementitious screed must prevent any risk of phase separation. Several additions, chemical or mineral, currently help ensure good stability of the screed; including welan gum, a kind of natural polysaccharide, which has proved very effective but still quite expensive [2] and lime that appears to have great stabilizing power [3], [4].

Compared to aerial lime (AL), natural hydraulic lime (NHL) provides additional strength due to its hydraulic reactivity [5], [6]. It has been found to enhance the stability of mixtures. However, the screeds have an average thickness of 5 to 6 cm and a high evaporation surface, which is likely to increase the cracking risk. Thus, understanding the impact of a natural hydraulic lime on the properties of cement-based mixtures is necessary to get durable products. Blended mortars of AL have been studied in literature. Most studies focus on the influence of the lime content or Binder/Aggregate ratio on the microstructure, mechanical

properties, pore structure and its influence on the capillary absorption and moisture transfer, and sustainability [7], [8], [9], [11], [11], [12]. It has been shown that AL accelerates cement hydration [7], [12]. Several explanations have been advanced that range from whether its physical presence allows direct nucleation on the lime grains [13] to its increase of the probability of homogeneous nucleation in the pores of the cement paste [14]. The addition of AL also causes an increase in porosity [6] that leads to a drop in stiffness [6] and strength [7], [15]. However, there is very little literature that deals with mortar mixtures based on cement and NHL.

This paper presents the results of a study carried out in order to understand the influence of the presence of NHL in binary mixtures with cement and ternary mixtures with cement and limestone filler, on fresh and hardened state behavior. Focusing on these mineral additions, this study attempts primarily to understand the mechanisms of action and the influence of NHL on cement-based mixtures, in substitution of cement. Then, a fixed volume of filler is added to the reference mortar to reach a minimum slump before the incorporation of lime, in order to investigate the influence of lime on cement mixtures in the presence of filler. The main engineering properties of self-levelling mortars were assessed, namely: the workability, setting time and early age shrinkage, strength and long-term drying shrinkage. These measurements were associated to laboratory analyses to understand how NHL influences the behavior of cement-based mortars with and without limestone filler.

2. Materials and methods

2.1. Materials

Portland cement CEM I 52.5 N was used for all the mixtures and its chemical composition and physical properties are given in Table I. The sand used in the mortar mixtures is siliceous sand. Its water absorption coefficient is 0.4% and its particle size distribution is presented in Figure 1. The mineral additions used are limestone filler (LF) and natural hydraulic lime (NHL). The chemical compositions and physical properties of these mineral additions are summarized in Table II. Their particle size distributions obtained using laser scattering technique are given in Figure 1.

The mineralogical composition of NHL used was taken from the supplier's data sheet [16], except for the content of Ca(OH)_2 which was determined by thermogravimetric analysis

(TGA) and which gave a value very close to that of the supplier. Note that even if NHL could contain small percentage of alite C_3S due to local overheat areas, the supplier's data sheet does not mention the presence of C_3S . The C_3S content of the NHL used in this study was actually so low that its mineralogical presence cannot be considered as significant. The same NHL 3.5 lime was used by Banfill et al. in another study [17], and the mineralogical composition presented does not show either the presence of C_3S . This is also the case of several authors who found only traces of C_3S in NHL lime [18][19].

Table I Cement properties

Portland cement CEM I 52.5 N				
<i>Chemical analysis (%)</i>				
CaO	SiO ₂	Al ₂ O ₃	Fe ₂ O ₃	SO ₃
63.7	19.8	4.4	2.2	3.2
<i>Compound composition of clinker (%)</i>				
C ₃ S	C ₂ S	C ₃ A	C ₄ AF	
68	11	8	7	
<i>Physical properties</i>				
Normal compressive strength (MPa)	d ₅₀ (µm)	BET (m ² /g)	Packing density	Water demand (L/kg)
61	15	0.77	0.56	0.25

Table II NHL and LF properties

NHL						
<i>Mineralogical analysis (%)</i>						
CaCO ₃ unburnt	Free Ca(OH) ₂	Insoluble	Hydraulic compounds			
			C ₂ S	C ₃ A	C ₄ AF	C ₃ S
25	26.2	9.6	35	0.5	0.5	trace
<i>Physical properties</i>						
d ₅₀ (µm)	BET (m ² /g)	Packing Density	Water demand (L/kg)			
10.5	3.6	0.42	0.54			
LF						
CaCO ₃	d ₅₀ (µm)	BET (m ² /g)	Packing density	Water demand (L/kg)		
96.9%	13.5	1.15	0.57	0.27		

The packing density of powders (cement, LF, NHL) was assessed from their water demand (Figure 2) by the equation (1). The water demand is measured using the flow spread test presented in [20], [21].

$$Packing\ density = \frac{1}{1 + \beta_p} \quad (1)$$

Where β_p (the intersection with the vertical axis) is the water demand of the powder, which represents the minimum quantity of water needed to initiate the flow.

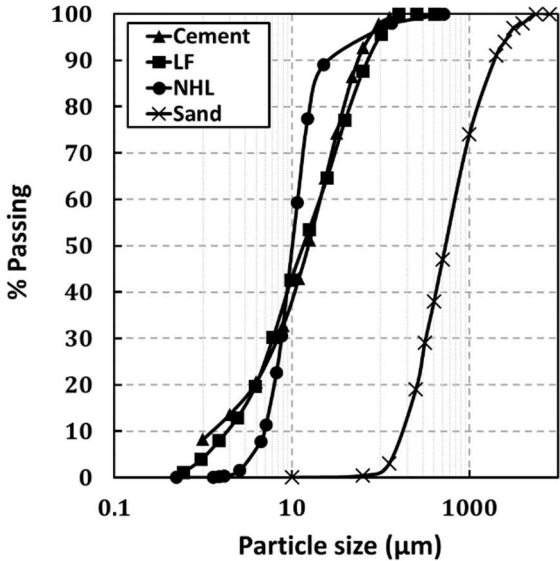


Figure 1 Particle size distributions

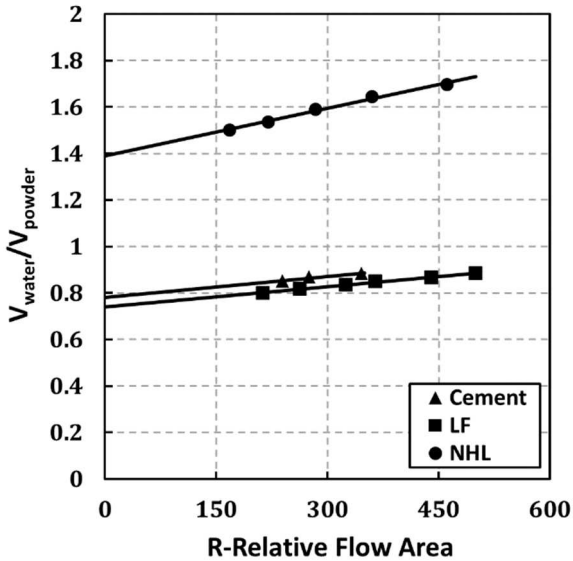
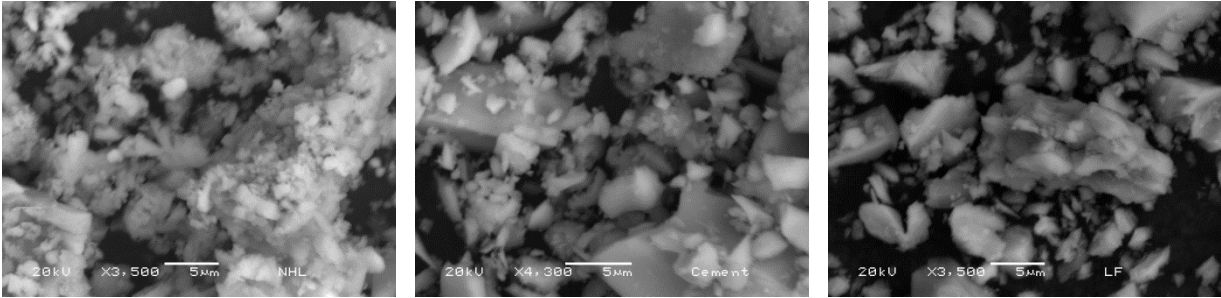


Figure 2 Water demand of powders

Cement and LF had approximately the same particle size distributions, specific surface area, and packing densities. NHL had significantly higher water demand, thus lower packing density. This can be attributed to the shape of NHL particles and their internal porosity (Figure 3), as the powder had approximately the same particle size distribution as cement and limestone filler, but significantly higher specific surface area from BET analyses (Table II). This property is useful for improving the stability of fluid mixtures with high water contents. The quantity of water fixed by 1kg of NHL, assessed from its water demand, was found to be twofold higher compared to that of 1kg of cement or LF (Table I and Table II). This allows ensuring a good homogeneity of the mixtures and avoiding excessive bleeding.



(a) NHL

(b) Cement

(c) LF

Figure 3 SEM images of (a) NHL, (b) Cement and (c) LF

2.2. Mix-design and preparation of mortars

This study was carried out in order to determine the influence of NHL and LF on the behavior of fresh and hardened mortars. This study initially focused on understanding the influence of NHL on the behavior of cement-based materials, by replacing a growing proportion of cement. Preliminary tests were performed by varying the paste volume of the reference mortar mixture allowing obtaining a target slump of 80 mm measured by mini-cone test (150 mm initial height). The reference mortar mixture with a water-to-cement ratio of 0.6 and a paste volume of 430 L/m³ was composed of Portland cement (CEM I 52.5 N), siliceous sand 0/4 and water. The cement was then replaced at different mass proportions with 12.5%, 25% and 50% of NHL, at a constant paste volume.

In the second step, a fixed volume of LF was added to the reference mortar prior to the incorporation of NHL. The aim was to assess the influence of NHL on cementitious mixtures in the presence of LF. A new reference mixture with LF was designed. The W/C ratio was fixed at 0.6 and the LF/C ratio at 0.6, and mixtures with different paste volumes were tested to reach a slump of 80 mm. The cement was then substituted with NHL using same mass proportions used previously i.e. 12.5%, 25% and 50% at a constant paste volume. The air content was taken equal to 40 L/m³ for all the tested mixtures.

All compositions were mixed according to the same mixing procedure. Sand, cement, LF and NHL (depending on the mixture composition) were dry mixed for 30s to ensure a homogeneous distribution of the mixture. Total amount of water was steadily added during 30s. The mortar was mixed for 90s, then scraped from the walls and bottom part of the bowl, and finally mixed for 90s.

Table III Composition of tested mortars

	Cement (kg/m ³)	LF (kg/m ³)	NHL (kg/m ³)	Sand (kg/m ³)	Water (kg/m ³)
Reference	467.1	-	-	1388.6	280.3
12.5% NHL	400.5	-	57.2	1388.6	280.3
25% NHL	336.5	-	112.2	1388.6	280.3
50% NHL	215.9	-	215.9	1388.6	280.3

100% NHL	-	-	401.3	1388.6	280.3
Reference LF	455.1	273.0	-	1152.8	273.0
LF+12.5% NHL	390.2	273.0	55.7	1152.8	273.0
LF+25% NHL	327.8	273.0	109.3	1152.8	273.0
LF+50% NHL	210.3	273.0	210.3	1152.8	273.0

2.3. Testing methods

2.3.1. Early age testing

Standard tests were associated to rheological measurements to understand the influence of NHL and NHL associated to LF on workability of cement-based materials. After mixing, the mortar slump was measured following EN 12350-2 and EN 12350-5. Rheological tests were performed on mortar's paste fraction. Two reference pastes with and without limestone filler (LF) and with water-to-cement ratio of 0.6 were actually considered. For each reference paste, cement was replaced by NHL with increasing mass proportions of 12.5%, 25% and 50%, while maintaining a constant $\{cement + NHL\}$ volume. Parallel plate rheometer was used to determine the rheological parameters. The distance between the two plates of the parallel plate rheometer has been fixed at 0.4 mm, and the shear rate used ranged from 0 to 50 s^{-1} . For each composition, 1 ml of cement paste was placed, using a syringe, on the bottom plate. A slowly increasing shear rate from 0 to 70 s^{-1} in 200 s was imposed. This first stage is needed to homogenize the specimen. As soon as the highest shear rate was reached, the plate stopped rotating. A cycle of increasing shear rate by 10 steps from 0 to 50 s^{-1} and back to 0 shear rate with another 10 steps was performed. At each step, the stress was measured and the computer recorded the average of the last five values. The rheological behaviors of the suspensions were identified by monitoring the evolution of the shear stress as a function of the shear rate. Measurements were performed just after mixing to avoid any influence of the hydration process.

The development of plastic shrinkage was measured as presented in [22] using a steel mold (Figure 4) with $70 \times 70 \times 280 \text{ mm}^3$ internal dimensions. The mortar is poured into an envelope formed of two reflective PVC plates, attached to a plastic sheet. The envelope is placed in the mold to reduce friction with the walls. The temperature is maintained at 20° C by circulating water in the lateral and lower faces. Two laser sensors are used for measuring the displacement of the plates entrained by the mortar during the shrinkage. The horizontal deformation allows calculating plastic shrinkage. Tests allowed drying on the top surface and

were performed in an air-conditioned room at a temperature of $20 \pm 1^\circ\text{C}$ and a relative humidity of $50 \pm 5\%$.

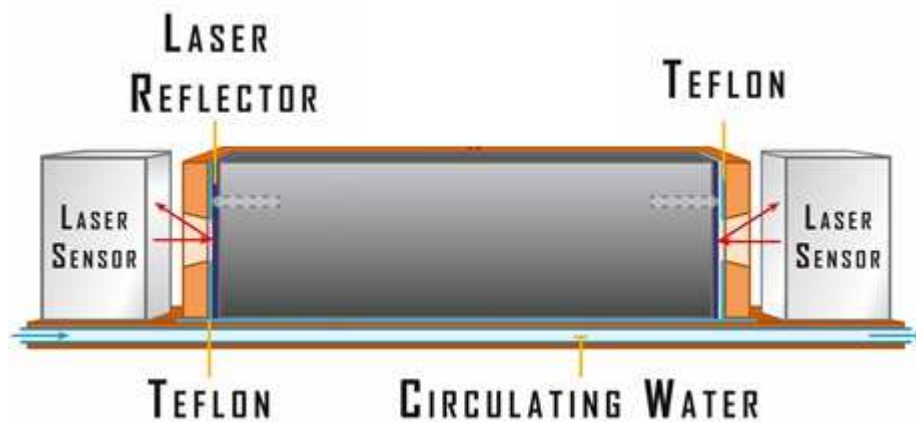


Figure 4 Plastic shrinkage testing device

Several properties were monitored in parallel to understand the evolution of plastic shrinkage: capillary depressions, weight loss, setting time, chemical shrinkage, hydration using an isothermal calorimeter, TGA/DTA, DSC, and elastic properties evolution at early age.

The capillary pressure was measured, as described in [23], using a porous ceramic cup placed horizontally in the middle of a cylindrical mold $\text{Ø}110 \times 70 \text{mm}^2$. In order to have the same environmental conditions as plastic shrinkage measurements, only the upper surface was subjected to drying. The ceramic cup was connected to a pressure sensor using a thin tube. The weight loss was monitored for all the mixtures using a mold with the same dimensions and drying conditions as the capillary pressure mold.

According to the European standard EN 196-3, the Vicat test was used to monitor initial and final setting time for all the mixtures. The test was conducted on two samples stored in water at 20°C in order to avoid the drying of the upper surface. The monitoring of setting was done by using an automatic device. The uncertainty on initial setting time was ± 0.5 h.

A TAM air isothermal calorimeter allows measuring the heat flow of mortar samples during hydration. The detailed procedure is described in [24]. Tests were conducted at a temperature of 20°C . The samples were 100 g in mass and cement was replaced with sand for the reference ampoule. The degree of hydration α , which is the fraction of cement that has reacted at a certain point in time and is often approximated by the extent of reaction ξ , was

calculated through equation (2), as the ratio of cumulative heat at time t - Q (t), to ultimate heat at the end of the reaction Q_{∞} [24].

$$\alpha(t) \approx \xi(t) = \frac{Q(t)}{Q_{\infty}} \quad (2)$$

The ultimate heat Q_{∞} was determined by plotting the cumulative heat as a function of $\frac{1}{\sqrt{t}}$. A linear evolution is obtained for small values of $\frac{1}{\sqrt{t}}$. The intersection of this linear function with the y-axis gives an estimation of Q_{∞} .

Thermal analyses were also conducted in order to determine the chemical activity of NHL and its effect on the nature and evolution of the hydration products. The evolution of portlandite and ettringite was monitored using different techniques: differential thermal analysis (DTA), thermogravimetric analysis (TGA), differential scanning calorimetry (DSC). The tests were performed on the paste fractions of reference and 50% NHL mortars (Table IV) at 3, 8 and 12 hours and at 28 days. About 150 mg of finely ground samples were heated from 20 °C to 1100 °C under nitrogen atmosphere, with a heating rate of 10 °C/ min.

Table IV Compositions of TGA-DTA and DSC tested pastes

	Cement (kg/m ³)	NHL (kg/m ³)	Water (kg/m ³)
Reference paste	1086	-	652
50% NHL paste	502	502	652

Portlandite Ca(OH)_2 decomposes between 400 and 500 °C. The measured weight loss $WL_{\text{Ca(OH)}_2}$ (%) due to the evaporation of water is used to calculate the amount of portlandite present using the molecular masses of portlandite (74 g/mol) and water (18 g/mol) (equation 3).

$$\text{Ca(OH)}_2(\%) = WL_{\text{Ca(OH)}_2}(\%) \times \frac{74}{18} \quad (3)$$

The values of portlandite measured for the 50% NHL paste have been corrected by removing the proportion corresponding to the Ca(OH)_2 initially provided by the NHL. A mass loss

equal to 2.03% was therefore always subtracted from the values measured for the 50% NHL pastes.

Chemical shrinkage measurements were carried out using the gravimetric method [25]. Just after casting, a sample of ~ 30 g of fresh mortar was poured into a 50-ml flask. A small orifice in the flask cap allows for a continuous water supply. The flask was held to a balance by a nylon thread and lowered in a water-filled tank. A mass value was taken every 5 minutes. From the recordings of the apparent mass of the flask, the amount of water penetrating into the paste and filling the porosities, generated by Le Chatelier's contraction, can be determined. The volume change was then calculated (equation 4).

$$\Delta V(t) = \frac{m_0 - m(t)}{V_{C0} \cdot \rho_w} \quad (4)$$

where $m(t)$ is the mass of both flask and sample recorded by the balance at time t , m_0 is the initial mass of both flask and sample, ρ_w is the water density and V_{C0} is the initial cement volume in the sample.

The evolution of elastic properties of mortars at early age was monitored by the FreshCon system [26][27]. The test procedure is presented in [22]. The evolution of dynamic properties (Poisson's ratio ν_{dyn} , shear modulus G_{dyn} and elastic modulus E_{dyn}) was obtained from the velocities of the compression waves and the shear waves [22]. The test was performed in an air-conditioned-room at 20 °C.

2.3.2. Hardened state testing

Compressive strength was measured on 40x40x160 mm³ mortar prisms according to the European standard EN 196-1 [28]. After mixing, samples were stored in the molds at 20 °C and 100% relative humidity during 24 h. Then the samples were demolded and water-cured at 20 °C until compressive strength test. Two mortar prisms were cut in two parts using an electric saw, thus four compressive strength tests were made at each age for each mortar composition.

Prismatic specimens 40x40x160 mm³ were prepared to measure total and autogenous shrinkage in accordance with the recommended practice of RILEM-AAC 5.2. The experimental setup used for drying shrinkage is described in [29]. After mixing, specimens were covered with a thin sheet of plastic to prevent water loss and maintained for 24h at

20 °C, and were then demolded for the shrinkage test. Tests were conducted in a conditioned room at 20 ± 1 °C and $50 \pm 5\%$ RH. Total shrinkage specimens were allowed to dry on lateral sides [42]. Autogenous shrinkage was measured at the same time on specimens covered with aluminum film to prevent evaporation. Since negligible autogenous shrinkage was measured, which is consistent with the relatively high W/C of the mixtures tested, only total shrinkage is presented in this paper.

3. Results and discussion

3.1. Workability and rheological properties

Figure 5 shows the slump obtained for each NHL substitution rate for mortars with and without LF. The incorporation of NHL decreases the workability of mortars containing or not LF. This negative effect is due to the lower packing density and larger specific surface area of NHL. Thus, more water is required to cover the entire surface, fill the voids between the grains, and therefore generate the flow. An exception to this is the 12.5% substitution rate in mixtures without LF where a 20% increase in slump was observed. It may be due to the optimization of the granular structure of the mix. In fact, when adding LF and/or NHL, the effect on the workability is the result of a competition between the high water demand of powders and the effect on the mixture packing density.

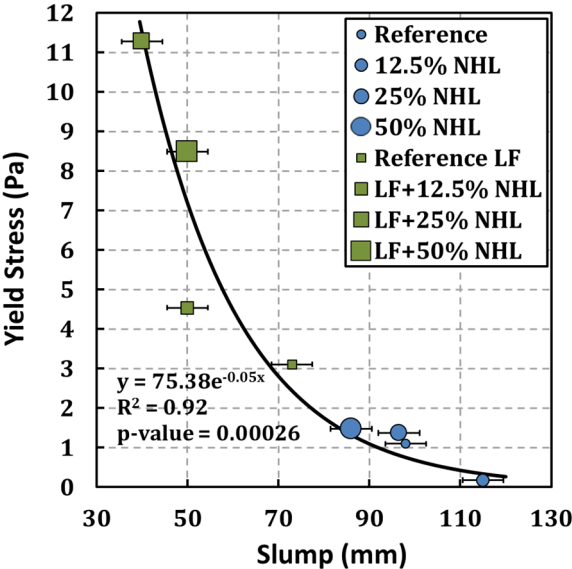


Figure 5 Yield stress vs. slump for tested mixtures

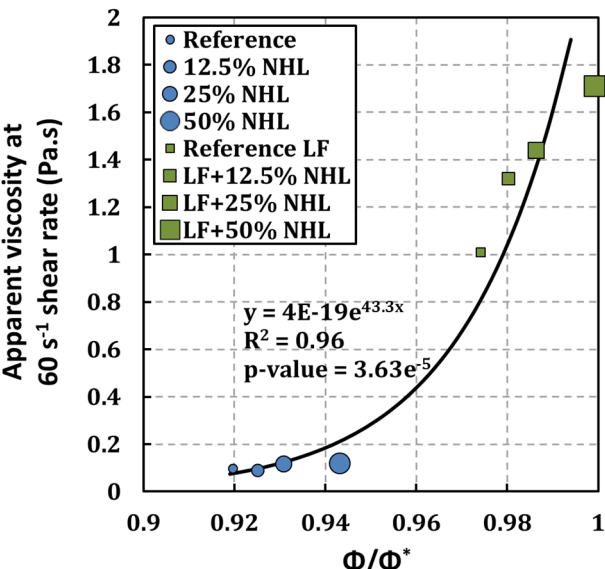


Figure 6 Relationship between apparent viscosity at 50 s^{-1} shear rate and relative solid concentration

Figure 7 shows the amount of fixed water (% of initial water content) defined here as the water demand of the mortar. It was assessed for each mixture based on the water demand of

its constituents. It can be seen that water retention increases with the addition of NHL, and that LF-mortars retain more water. The remaining amount of free water available to participate to the flow thus decreases.

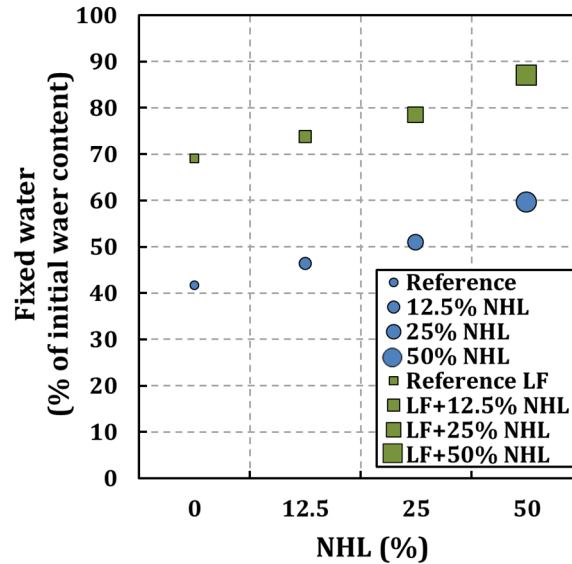


Figure 7 Fixed water by mixtures with increasing NHL content

A rheological study was conducted on mortars' pastes fractions with and without LF **with increasing NHL substitution rate**. The apparent viscosity, defined as the ratio of measured shear stress to applied shear rate at a specific shear rate [30], was calculated at 50 s^{-1} shear rate. At this shear rate the evolution of the viscosity has reached a pseudo-Newtonian behavior. Figure 5 and Figure 6 show that for mixtures without LF, **increasing NHL contents** (exception made of 12.5% substitution) lead respectively to slight increase in yield stress without affecting the viscosity. In the case of LF mixtures, the incorporation of NHL leads to a significant increase in the yield stress and a slight increase in viscosity (Figure 5 and Figure 6). This corroborates the results found by other researchers showing that the viscosity and the yield stress increases with the specific surface area [31], [32]. Mixtures containing LF actually generate a larger specific surface area and require a larger volume of water to generate the same flow as mixtures without LF. Moreover the incorporation of NHL results in an increase of the total specific surface area. The optimum obtained in the yield stress curve for 12.5% NHL could be due to a higher packing density.

It should be noted that the yield stress values measured for the various compositions are the result of the competition between two phenomena: i) the greater water demand generated by the addition of NHL and which leads to the increase of the yield stress [33], [34], and ii) the

decrease in the amount of cement following its substitution by NHL, and the induced reduction of colloidal interactions which are dominated by Van der Waals force and which reduce the yield stress [34], [35]. Bentz et al. [30] have studied the rheological parameters of blended cement/fly ash pastes and found that yield stress is dominated by the particle density of the cement component, with the fly ash acting as a diluent that effectively decreases the cement particle number density, leading to a decrease in yield stress. The non-linearity observed between LF+25% NHL, with a higher yield stress, as compared to LF+50% NHL may reflect the preponderance of decreased interparticle interactions on the higher water demand.

The slump of mortars was determined from mini-slump test. The mortar can flow if the stress due to the weight of the mortar cone is higher than its yield stress. The plot of yield stress vs. slump (Figure 5) shows that higher yield stress of the paste generally resulted in a lower slump of mortar [33]. This is due to intergranular friction during mortar shear. For a given water content, the intergranular friction increases as the packing density of the mixture decreases. The same relationship between yield stress and slump has already been reported in literature in the case of cement pastes [33], [35]. This global trend, however, does not allow concluding on a correlation between the two properties. The LF + 25NHL, LF + 50NHL and LF + 12.5NHL mixtures actually exhibited very similar slump values for significantly different yield stress values, which shows that there is no a clear correlation between the yield stress of paste and the slump of mortar (at least concerning these experimental results). The results obtained for the LF + 25NHL, LF + 50NHL and LF + 12.5NHL mixtures indirectly show that the behavior of mortar does not only depend on the properties of cement paste. Indeed, interactions between the paste and sand particles have a significant influence on mortar behavior.

Viscosity is closely linked to the relative concentration of the mixture, defined as the ratio between the volumetric proportion of solid materials Φ and its maximum packing density Φ^* calculated using the *Compressible Packing Model* developed by De Larrard [36], [37]. Figure 6 shows the correlation between the apparent viscosity at 50 s^{-1} shear rate and relative solid concentration Φ/Φ^* . It can be seen that the lower the relative solid concentration, the lower the apparent viscosity. The viscosity is actually related to the flow of water in the porosity of the granular system [37]. For a given solid fraction, the higher the packing density, the lower the ratio Φ/Φ^* , thus the water then flows more easily, which leads to a low apparent viscosity.

3.2. Hydration and volume stability

Setting time and shrinkage are major engineering properties of self-levelling mortars. Setting time should allow the transport and placement of the mortar without affecting its workability. The high evaporation surface of screeds generates plastic shrinkage. As soon as the material begins to harden restrained shrinkage is likely to develop, thus setting also influences the cracking risk. Both properties, i.e. setting and plastic shrinkage, were assessed simultaneously for all the studied mixtures and other tests were performed in order to understand their evolution.

The initial setting time of the studied mortar mixtures can be correlated with the evolution of other physical and mechanical mortar properties at early age [23]. The results presented in section 3.1 showed that the specific surface area (SSA) of powders had a major influence on the early-age behavior of studied mortar mixtures. In Figure 8 the initial setting time is plotted as a function of the total specific surface area available per mass of cement S_{tot} (calculated by equation 5) which allows taking the fineness and amount of the powders into consideration.

$$S_{tot} = \frac{S_{LF} \cdot m_{LF} + S_{NHL} \cdot m_{NHL}}{m_C} \quad (5)$$

Where S_{LF} and S_{NHL} are the specific surface areas respectively of LF and NHL, and m_{LF} , m_{NHL} and m_C are the massic contents of LF, NHL and cement respectively in the mixtures.

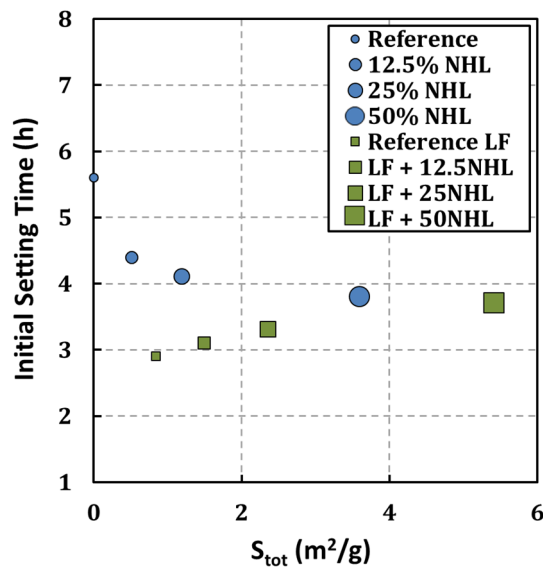


Figure 8 Initial setting time vs. total surface of contact for tested mortars

The replacement of cement by NHL and/or LF resulted in both cases in a significant reduction in initial setting time compared with the plain Portland cement mixture. As cement replacement increases, two parameters produce adverse effects, namely: lower clinker content and higher specific surface area. With increasing substitution rates, a higher number of C-S-H nuclei is created on the surface of limestone [38] until an optimum surface is reached beyond which the incorporation of the powder no longer has an accelerating effect, and can influence the setting by delaying the creation of connectivity between solid (Figure 8). This can be attributed to the influence of water-to-cement ratio and the percolation threshold effect on the development of mechanical properties [39]. At high cement replacement, NHL and LF actually show the same behavior, whereas for the same lower S_{tot} values LF lead to significantly lower setting times (Figure 8). LF-based mixtures actually had higher relative solid concentration Φ/Φ^* (see 3.1) thus the percolation threshold is reached earlier. However setting is a complex process resulting from both chemical and microstructural evolutions. Moreover the influence of mineral additions on early age properties does not only depend on their specific surface area, but it results from the combination of the filler effect, the pore solution chemistry and their surface characteristics [40], [41]. Isothermal calorimetry, TGA, DSC, and ultrasonic monitoring were performed on the same materials in order to understand the influence of studied mineral additions on the main phenomena involved in the first stages of hydration and hardening.

As the hydration reactions are exothermic, the monitoring the heat flux allows to understand the effect of NHL on hydration of cement-based materials. Since the exothermic peak of the 100% NHL mortar has a relatively low magnitude and approximately the same position (Figure 9), it can be concluded that NHL hydration has no direct consequence on the heat flow from 1h. Therefore, in all the mixtures, the thermal flux has been normalized by the amount of cement in the sample.

The heat flow curves plotted on Figure 9 and Figure 10 show the typical stages of Portland cement hydration, with the initial, induction, acceleration and deceleration periods. The latter two periods are often called the “main period” as they are mainly influenced by the silicate reaction corresponding to the hydration of alite (C_3S). Another peak can be distinguished as a shoulder on the decreasing part of main peak. It corresponds to the “sulfate depletion peak” as described by Lerch [42] and confirmed by the works of Hesse et al. [43] and Jansen et al. [44]. This aluminate peak corresponds to acceleration of C_3A dissolution as soon as the

sulfate carrier (gypsum for example) has completely dissolved. However ettringite has been reported to develop at a significant rate before this aluminate peak.

The comparison of Figure 9 and Figure 10 shows a significant shift of LF peaks towards earlier ages. The accelerating effect of LF on cement hydration is actually well known [45] and consistent with setting data (Figure 8). Schöler et al. [41] studied the influence of several supplementary cementitious materials on the first stages of hydration and they actually found that limestone lead to the lower degree of oversaturation with respect to C-S-H and this was related to the presence of more C-S-H nuclei formed on the surface of limestone particles. Figure 9 shows heat flow profiles for the cement mortars with increasing NHL substitution rate. The hydration of the mixtures containing NHL is accelerated compared to the reference (plain) mixture as indicated by the progressive leftward shifts and the earlier apparition of the hydration peak and the induced short dormant period. In the case of LF mixtures, the acceleration of hydration is also observed, but to a smaller extent (Figure 10), as the main effect was probably due to limestone. This is consistent with the setting results of Figure 8, as the increase of NHL content in LF-based mortars did not result in lower setting time.

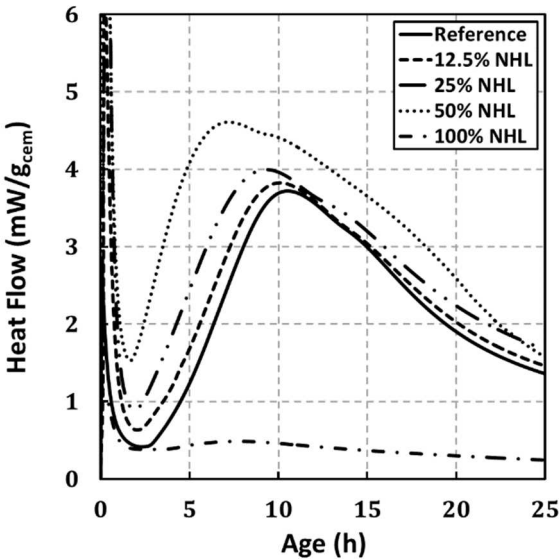


Figure 9 Heat flow as a function of specimen age assessed for NHL mortars without LF

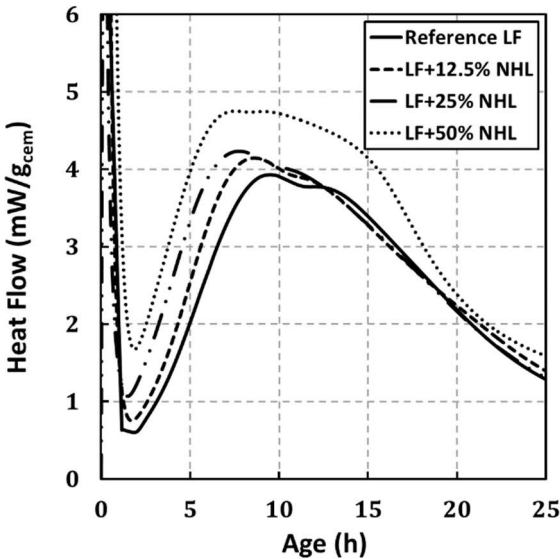


Figure 10 Heat flow as a function of specimen age assessed for NHL mortars with LF

The acceleration effect of NHL on cement hydration can have two origins: an influence on saturation indices for C-S-H and for C₃S through changes in the chemistry of pore solution, or new nuclei due to the presence of NHL particles [13]. The results of this study and previous works do not allow excluding one of this two effects.

Since, apart from the first thermal peak observed, no significant hydration reaction of the NHL is visible during the first hours, its accelerating effect can be considered similar to the accelerating effect due to aerial lime. The hydration acceleration in the case of blended mortars of cement and aerial lime has been reported in the literature [7], [12], [14]. The acceleration of hydration is most likely due to nucleation on NHL grains or a promotion of homogeneous nucleation probability in the pores. Moreover, the effect of the NHL proportion is observed whereas the concentration of the pore solution is the same for all samples after the first NHL dissolution peak [13].

The NHL particles are partly dissolved in the solution, which modifies its calcium concentration and its pH. These two parameters have direct influence on the main factor for alite dissolution which is the degree of undersaturation with respect to C_3S . This variation of the concentrations could induce a change in the kinetics of the silicate phases dissolution and the aluminate precipitation. It has been shown that a high initial $Ca(OH)_2$ concentration leads to a decrease in the number of CSH nuclei [46], but Schöler et al. [41] showed that higher calcium concentrations do not lead to a systematic decrease of the reaction rate of C_3S and C_2S .

TGA and DSC measurements were conducted on the reference and the 50% NHL pastes to better understand the underlying mechanisms of the observed evolutions of setting and plastic shrinkage. Figure 11 is a plot of the time-evolution of the $Ca(OH)_2$ content in the reference and 50% NHL pastes. Note that the values shown for the 50% NHL paste are corrected by removing the proportion of $Ca(OH)_2$ initially brought by NHL. It appears that during the acceleration period, the rate of $Ca(OH)_2$ production is higher in the mixture with NHL than in reference paste. This confirms that NHL has an influence on dissolution and precipitations processes related to the hydration of C_3S .

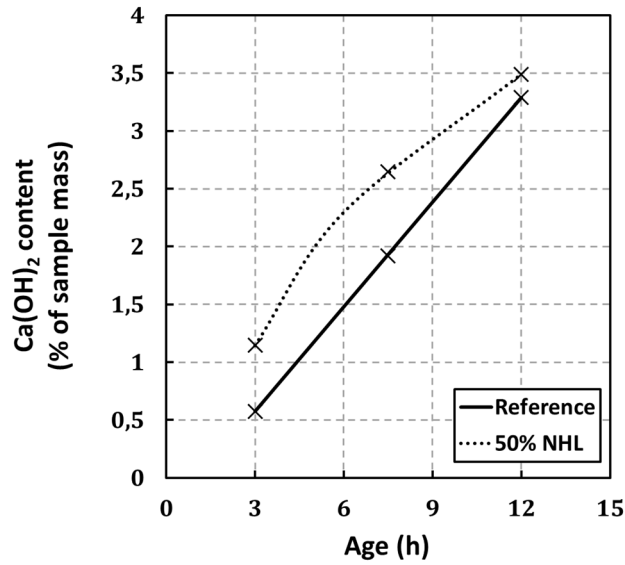


Figure 11 Evolution of the portlandite content

In order to monitor the development of ettringite, the consumption of the setting regulator by the mineral phases of clinker C_3A and C_4AF to produce ettringite was measured with DSC. The evolution of the endothermic peak located between 120 and 160°C is inversely correlated to the production of ettringite [47]. Figure 12 shows that this peak vanishes after 12h and 8h for the reference and 50% NHL paste respectively, which suggests that ettringite developed faster in the presence of NHL. This is consistent with the displacement of the sulfate depletion peak observed in Figure 9. It actually became visible on heat flow curves at 9 hours for 50% NHL mixture and 13 hours for the reference mixture.

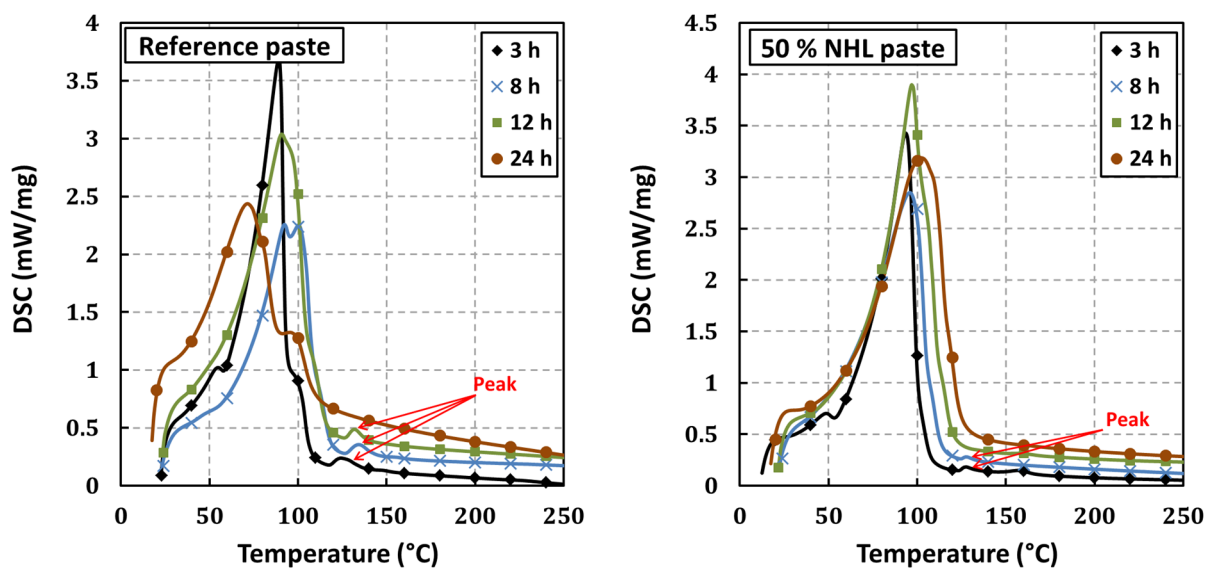


Figure 12 Thermal analysis of reference and 50% NHL pastes by DSC

To determine the volumetric changes induced in the mortar when adding NHL, measurements of chemical shrinkage have been carried out. Chemical shrinkage is the volumetric contraction of the material under the effect of hydration [48]. This test provides the total voids volume formed in the material because of the sole action of the hydration. Figure 13 shows the results obtained for the reference mortar and the 50% NHL mortar. The overall volume change was the same as that measured for the reference, meaning that the introduction of NHL did not significantly affect the hydration products volumes at early age. However, a small plateau is observed for NHL mortars; it most likely corresponds to the early expansion due to the rapid formation of hydration products during the acceleration period as shown by isothermal calorimetry, TGA and DSC results.

The NHL, not participating directly in hydration, its contribution can be considered similar to that of the filler. Apart from the dissolution of NHL, LF and NHL are therefore powders whose effect on the hydration is limited to the creation of additional nuclei of formation of hydration products due to their high specific surface area. In spite of significantly higher SSA, NHL had lower accelerating effect than LF. This suggests that NHL particles had different surface properties and that the dissolution of NHL particles during the acceleration period had an influence on nucleation and saturation indices in the pore solution.

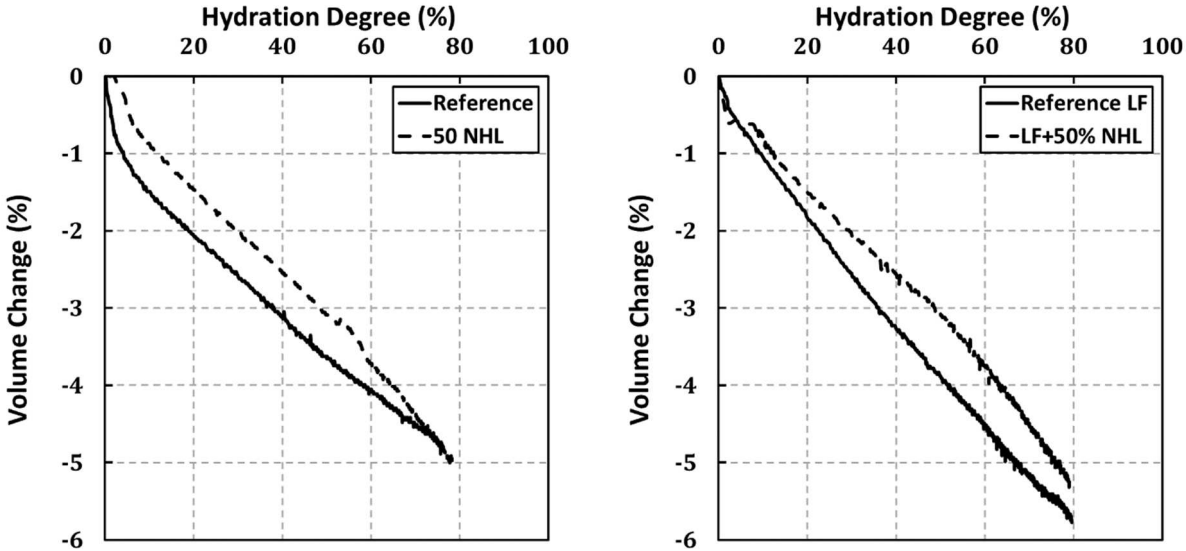


Figure 13 Chemical shrinkage vs. Hydration degree for mortars with and without LF

It should be noted, however, that the increase in NHL proportion delayed initial setting of mortars with LF (Figure 8), whereas the monitoring of heat flow by isothermal calorimetry

showed an acceleration of hydration (Figure 9 and Figure 10). In order to understand the effect of NHL on setting and hardening processes, the evolution of the shear modulus was monitored. For all the mixtures, the shear modulus G starts to develop when the first hydration products are formed, filling up the pore space and creating a denser structure. Thus, an increase in shear modulus will cause a growth in the S-wave velocity and the penetration resistance to Vicat needle.

The experimental results of the study allow investigating the correlation between the hydration degree and the shear modulus. It can be seen from Figure 14 that for the same degree of hydration, mixtures containing LF develop a higher shear modulus. The acceleration of the initial setting and of the hydration caused by the presence of the LF was reported in the literature [49]. LF being chemically inert, this effect is essentially due to nucleation on LF particles. Figure 14 also shows that for mixture with NHL, a 10% reaction degree was reached without being accompanied by any significant development of the shear modulus. This suggests that hydration reactions did not directly lead to the formation of a continuous solid microstructure. The higher apparent W/C ratio and the higher mineral addition proportion in mixtures containing NHL can explain this. At high W/C ratio and high addition contents, a higher quantity of hydration products is required in order to reach the percolation threshold. In the contrary case, anhydrous grains are closer to one another, and then only a small quantity of hydration products needs to be formed in order to achieve percolation [39].

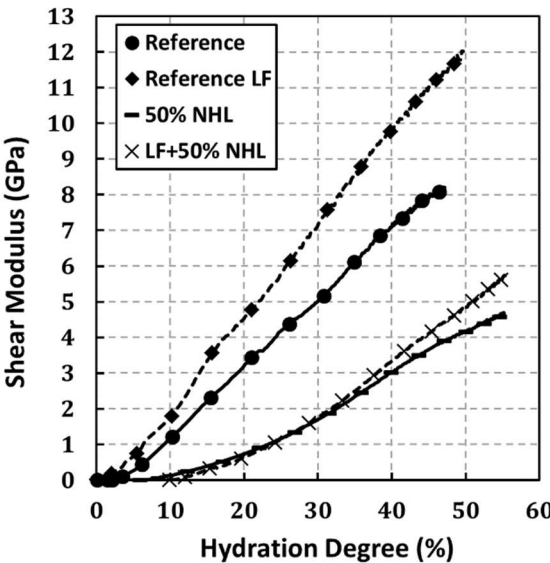


Figure 14 Shear modulus as function of the hydration degree

Drying of concrete surfaces during the first hours after casting may lead to a very pronounced water loss due to the high permeability of fresh concrete. The water loss when concrete is still plastic results in increased deformations, referred to as plastic shrinkage [50]. Figure 15 is a plot of the 24-hour plastic shrinkage magnitude for mortars with increasing substitution rate of cement by NHL. The addition of NHL led to a considerable reduction of the plastic shrinkage magnitude.

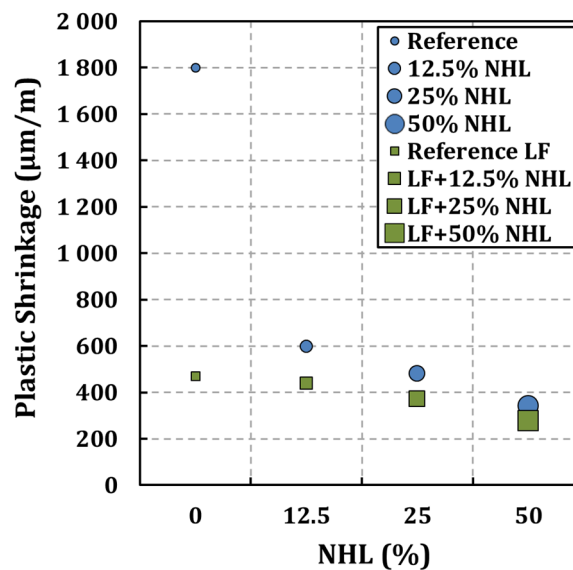


Figure 15 Plastic shrinkage of mortars with increasing NHL content

Several assumptions can be put forward to explain the effect of the NHL on the development of plastic shrinkage. The authors distinguished three sets of mechanisms from the results available in literature on Shrinkage-Reducing Admixtures (SRAs).

i) Mechanical effect. In the same time as shrinkage develops the material begins to harden. The NHL could have affected the hydration kinetics and thus accelerated the mortars' final setting time, which results in higher stiffness allowing the mixtures to counteract the deformations caused by capillary tension. A recent study of the authors has shown that the magnitude of plastic shrinkage is conditioned by drying rate and setting time. Thus accelerated drying results in higher shrinkage as this can develop before setting [51].

ii) Physical effect. NHL could actually influence the drying rate thereby maintaining a high internal relative humidity and reducing the surface tension of solutions in the pores. This should reduce the capillary stresses and therefore the shrinkage [52]–[55]. Internal curing

could be associated to the internal porosity of NHL particles, and reabsorption of bleeding water has also been reported to mitigate the development of self-desiccation shrinkage.

iii) Chemical effect. Some SRAs cause crystallization pressures and therefore an increase in apparent volume, or modify the relative proportions of hydration products and thus the chemical shrinkage. In this case the addition of NHL would result in a period of expansion which induces a compressive stress in the system and provides a considerable benefit in shrinkage mitigation [52], [56].

These assumptions, which came as natural speculations, are checked in this section in order to identify the possible mechanisms of plastic shrinkage reduction occurring in the presence of NHL.

Plastic shrinkage develops when the mortar is still in its plastic stage. The plastic stage is the period between casting and initial setting. When setting begins, the process of hydration allows the formation of a continuous solid structure and therefore the rise in stiffness. The strain capacity thus decreases strongly [57]. When the setting is completed, the mortar has developed sufficient stiffness to reduce the strains caused by the capillary forces developing in the pores. It would therefore be logical to think that the acceleration of the hydration caused by the presence of LF and NHL allows rapid formation of a solid skeleton, which mitigates the development of deformations due to plastic shrinkage. Figure 16 shows a correlation between the time of stabilization of the plastic shrinkage and the final setting time. The final setting actually occurred well before the stabilization of the plastic shrinkage, deformations therefore developed after the formation of the solid, which could cause cracking. A linear relationship between the final setting time and the plastic shrinkage stabilization time can be drawn for mortars with LF, but there is not a monotonic evolution as that observed for plastic shrinkage magnitude. The shrinkage of mixtures without LF developed for periods of very variable durations while the end of setting took place at approximately the same time. Thus the acceleration of setting is not sufficient on its own to explain the observed reduction of shrinkage magnitude.

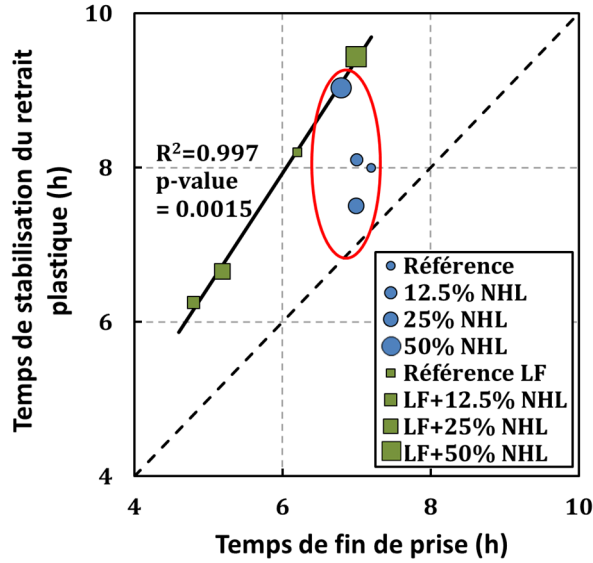


Figure 16 Plastic shrinkage stabilization time vs. final setting time for tested mortars

The main mechanism leading to plastic shrinkage is the development of drying induced capillary suction in the pore fluid [58], [59]. Capillary pressure gradient actually appears between the surface and the bulk [60] and cause the solid skeleton to compress, which induces the shrinkage. Capillary pressure p is related to the surface tension of the pore solution γ , to the pore radius r and to the internal relative humidity according to Kelvin-Laplace equation (6)

$$p = \frac{2\gamma}{r} \cos(\theta) = \frac{-RT\rho_e \ln(h)}{M} \quad (6)$$

where p , R , T , M , ρ_e , h , γ , r and θ : denote capillary stress, universal ideal gas constant, temperature, molar mass of water, water density, humidity, surface tension of pore fluid, pore curvature and contact angle, respectively.

As the internal relative humidity or pore radii decreases, the capillary pressure increases. In addition, a high surface tension generates a high capillary pressure. Transport of water in fresh mortar and its evaporation from the surface is, therefore, of key importance in understanding the plastic shrinkage. In order to check whether the presence of NHL affects the drying kinetics, the mass loss of the mixtures was monitored. The Figure 17 shows the measured mass losses in the case of mortars without LF. Note that in the presence of LF the results are globally the same during the first 4 hours, when the main differences can be observed on plastic shrinkage evolution. Whereas these mixtures showed quite different kinetics of plastic shrinkage, the evaporation rates were approximately the same. This

suggests that the NHL did not influence the drying kinetics, which would have been the case if NHL had significantly modified the surface tension of pore solution γ .

It is well known than in the case of cementitious materials with a high ratio of water to binder in sealed condition, swelling can occur if there is bleeding. During the consolidation, surface water is reabsorbed by the material, causing swelling [61]. Our tests were carried out under drying conditions; the film of bleeding water, which appeared on the surface, disappeared rapidly after about an hour. Moreover the water initially fixed by powders increased with NHL proportion (Figure 7) thus the absorption of bleeding water cannot be expected to be a major parameter, which is confirmed by drying rates (Figure 17).

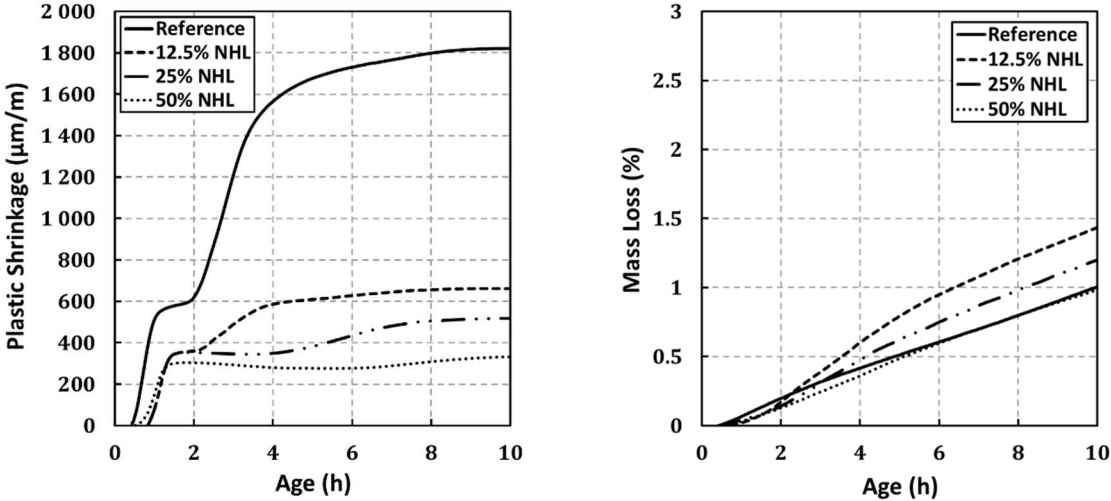


Figure 17 Plastic shrinkage and mass loss for mortars without LF

Figure 18 shows the capillary depressions of mortars without LF. It appears that the curves corresponding to the four mixtures are superimposed during the first 8 hours whereas significant differences are observed in the evolution of plastic shrinkage. Since capillary depression is directly related to internal relative humidity (equation 6), the observed evolutions of capillary depressions confirm that NHL does not affect the moisture state's evolution of the material at early age.

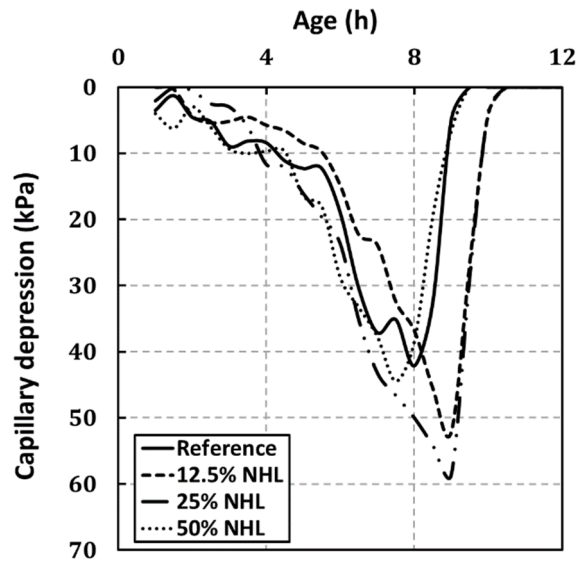


Figure 18 Evolution of capillary depression for mortars without LF

Under the conditions of the test, the reference mixture showed a plateau in the development of shrinkage at 1h. During the same time period, the mortar with 50% NHL showed an expansion (Figure 17). This expansion period makes it possible to compensate for the shrinkage and results in a sharp reduction in plastic shrinkage [62]. The expansion period can be clearly observed by plotting the difference between the shrinkage curve obtained for the reference and that obtained for the 50% NHL mixture (Figure 19).

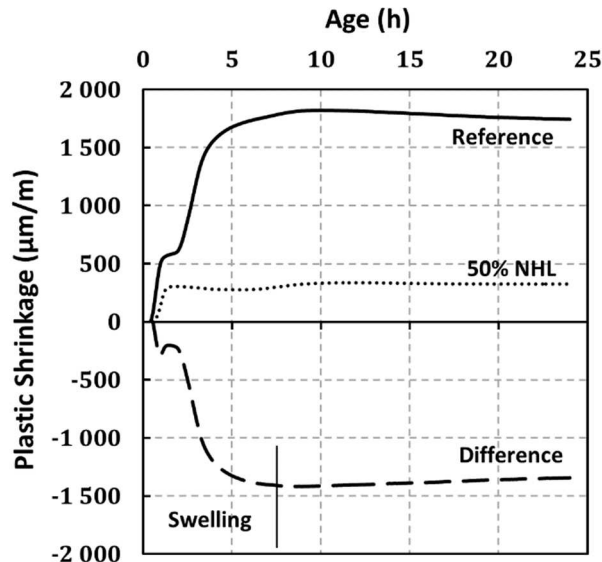


Figure 19 Expansion period for 50% NHL mortar

Since swelling is not the consequence of difference in volume of chemical products (Figure 13), the mechanism that causes swelling is thus due to a faster precipitation of hydration

products. The growth of ettringite crystals in the fine pores of the matrix or “crystallization pressure” leads to macroscopic expansion. If crystals are formed in the capillary pores, they do not cause expansion, whereas if they develop in the gel pores, they grow on the adjacent particles and thereby cause expansion [63], [64]. The stresses due to crystallization, i.e. the difference between the crystal and the liquid pressure $\sigma_c = p_c - p_l$, actually depend on pore radius (equation 7).

$$p_c - p_l = - \frac{2\gamma_{cl}\cos(\theta)}{r_p} \quad (7)$$

where γ_{cl} is the crystal surface energy at the crystal/liquid interface, for a crystal growing inside a cylindrical pore of radius r_p with a contact angle θ .

The crystallization pressure exerted on the surrounding pore wall [65], [66] can be expressed by equation (8).

$$\sigma_c = \frac{RT}{v_c} \ln\left(\frac{Q}{K}\right) \quad (8)$$

where R , T , and v_c are respectively gas constant, absolute temperature, and molar volume of the crystal; Q/K is the supersaturation for a given crystal.

According to the crystal growth pressure theory, the driving force for the crystallization pressure is the supersaturation of the pore solution. In the case of ettringite the ratio is given by equation 9.

$$\frac{Q}{K} = \frac{(a_{Ca^{2+}})^6 \cdot (a_{Al(OH)_4^-})^2 \cdot (a_{OH^-})^4 \cdot (a_{SO_4^{2-}})^3 \cdot (a_{H_2O})^{26}}{K_{ettringite}} \quad (9)$$

The expression of the supersaturation for ettringite shows that Ca^{2+} and OH^- concentrations are major parameters as they are respectively to the power 6 and 4, and these ions are released by the dissolution of NHL. It has actually been reported in the literature that ettringite is expansive in the presence of lime [67]. Min [67] shows that if the lime is absent, the crystals of ettringite are large, coarse, and do not cause swelling, whereas those formed in a saturated lime solution are fine, prismatic or granular, and grow around the aluminum-bearing particles.

These mechanisms are in agreement with the assumption that the observed expansion period of NHL-cement mortars is related to the rapid formation of hydration products (particularly ettringite and portlandite) which apply crystalline pressures on the pore surfaces [68], [69].

Ettringite is actually not the only product able to produce crystallization pressure [62]. TGA showed a higher rate of portlandite formation during the first hours of hydration (Figure 11). Expansion is not only due to the formation of expansive products but also to the lower stiffness of the cementitious matrix. DSC analyses showed that ettringite appeared earlier (Figure 9 and Figure 12), while the elastic modulus was still relatively low (Figure 14).

The direct confirmation of this assumption would require measures of ionic concentration in pore solution and the calculation of saturation indices [41], [62] but all the data gathered in this experimental study allows to think that this is the most probable explanation of expansive stage observed in plastic shrinkage evolutions.

3.3. Effect on hardened state:

The Figure 20 shows the effect of cement substitution by NHL on the compressive strength at 28 days for mixtures containing or not LF. The incorporation of the NHL resulted in a drop in compressive strength. This adverse effect was largely reported in the case of blended cement and aerial lime mortars [7], [70]. In the case of the NHL the effect does not vary much, except in the case of mixtures with LF where an optimum was observed at 12.5% substitution rate.

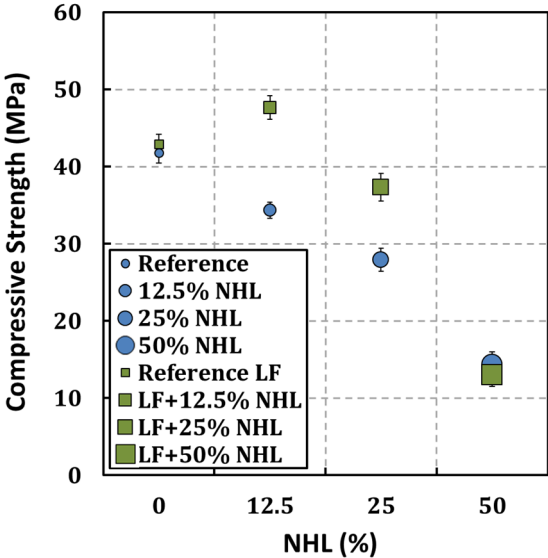


Figure 20 Compressive strength as function of the NHL proportion

This effect of mineral additions in replacement of cement has been reported in the literature [71]. The compressive strength of a mortar containing a given proportion of a mineral addition is represented by the combination of three different effects [71], each of them is quantified as a fraction of the strength (7).

$$f_{tot} = f_{dilution} + f_{physical} + f_{chemical} \quad (7)$$

- $f_{dilution}$ is the strength related only to the amount of cement in the mixture, without considering any effect of mineral admixture, except dilution. An increase in the proportion of mineral admixture involves a decrease in the amount of cement and consequently lower compressive strength compared to a reference without mineral admixture.
- $f_{physical}$ is the contribution to compressive strength due to the physical effect of the mineral admixture: filler effect or heterogeneous nucleation. The filler effect makes it possible to fill the voids of the mixture, thus modifying the initial porosity, which leads to an improvement in the packing density and therefore to a higher strength. Heterogeneous nucleation is a physical process related as seen before to the nucleation of hydration products on small mineral particles. It favors cement hydration, thus induces an increase in the compressive strength. This physical effect depends essentially on the fineness and the amount of the powders used [24], [45], [49].
- $f_{chemical}$ is a gain of strength related to the pozzolanic reaction. Its effect is noticed after periods of a few days to several months, depending principally on the type and chemical composition of the addition.

The substitution of cement by NHL corresponds to a decrease in cement content. This is naturally accompanied by a decrease in compressive strength ($f_{dilution}$) compared to that of the reference mortar, which justifies the drop in strengths observed in Figure 20.

In order to measure only the compressive strength due to the dilution effect, it is necessary to use a chemically inert mineral addition, composed of particles large enough to consider that heterogeneous nucleation is not significant. According to the literature [4], the mean diameters of NHL (10 μ m) and LF (12 μ m) are not large enough to exclude any heterogeneous nucleation effects. Thus, the presence of NHL and LF contributes by physical effect to the gain of strength ($f_{physical}$).

The contribution of the presence of NHL and LF to compressive strength by chemical effect ($f_{chemical}$) can be considered as negligible here. LF is actually a mineral addition considered as chemically inert, and on the other hand, the NHL hydration is not significant during the first 28 days. The strength increase in the first days is due to the hydration of the hydraulic

compounds, and mainly of the C_3S contained primarily in the cement and in small proportions in the NHL [6]. The contribution of the hydration of the C_2S present in large proportion in the NHL to the strength is significant only from 28 days [70]. This was confirmed by 28-day TGA measurements conducted on the reference and the 50% NHL pastes (Figure 21). It appears that the reference paste and 50% NHL paste contain respectively 9.5% and 4.4% of $Ca(OH)_2$. Note that the $Ca(OH)_2$ content in the 50% NHL paste is corrected by removing the proportion of $Ca(OH)_2$ initially brought by NHL. As the $Ca(OH)_2$ in reference paste is only produced by cement hydration, the cement's content in the 50% NHL paste should yield 4.4% $Ca(OH)_2$, which corresponds exactly to the measured value (when removing the proportion of $Ca(OH)_2$ initially brought by NHL).

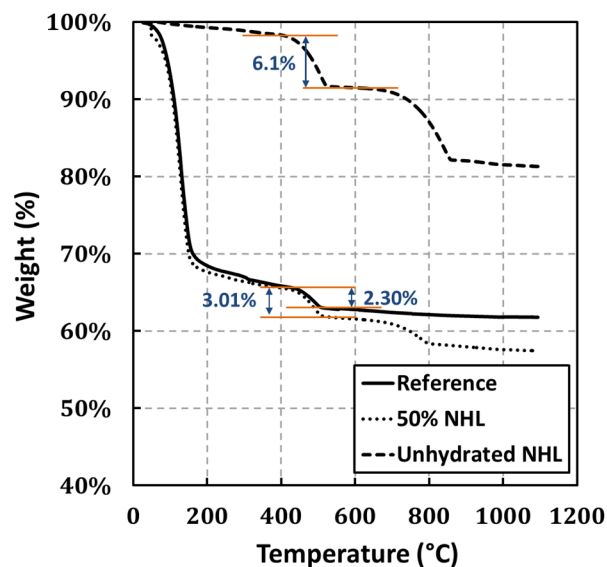


Figure 21 Thermogravimetric analyses of unhydrated NHL and reference and 50% NHL pastes

Thus, during the first 28 days, the mineral additions participate in the increase of compressive strength mainly by the physical effect. As pointed out before, this physical effect depends essentially on the specific surface and the amount of the powders used [24], [45], [49]. This can be proposed to account for the better strengths obtained in the case of mixtures with LF and the optimum compressive strength obtained for a 12.5% NHL substitution rate. The powder obtained by mixing NHL and LF has a better fineness, thus allowing a better contribution to the increase in strength. The optimal replacement rate of 12.5% NHL in the presence of LF can be explained by obtaining a mixture with optimal total packing density or by obtaining an optimal specific surface area to clinker content ratio.

The drying shrinkage was represented using the hyperbolic equation (8) introduced by Torben & al. [72] since it allows better fitting of experimental data.

$$\epsilon_{dry} = \frac{t}{t+N_s} \epsilon_{\infty} \tag{8}$$

The two parameters, ϵ_{∞} ultimate drying shrinkage and N_s time to reach half of the ultimate drying shrinkage, were determined from the experimental data to minimize the mean square error. The evolution of shrinkage strain is then described by combining two parameters: magnitude and kinetics. It can be seen from Figure 22 that as the rate of cement substitution by NHL increased, the drying shrinkage decreased.

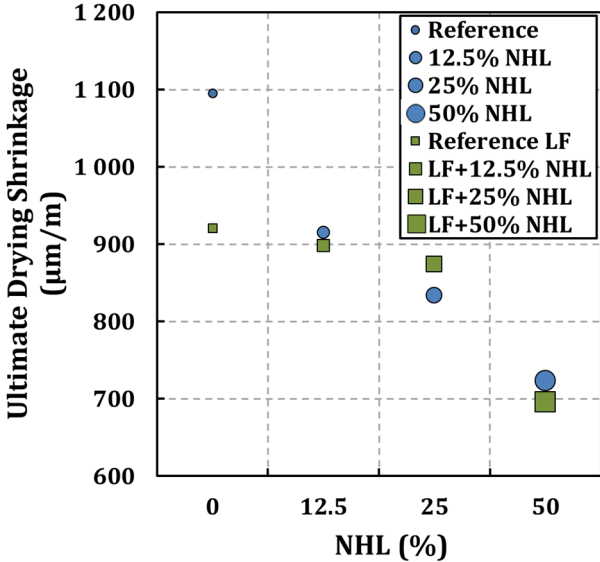
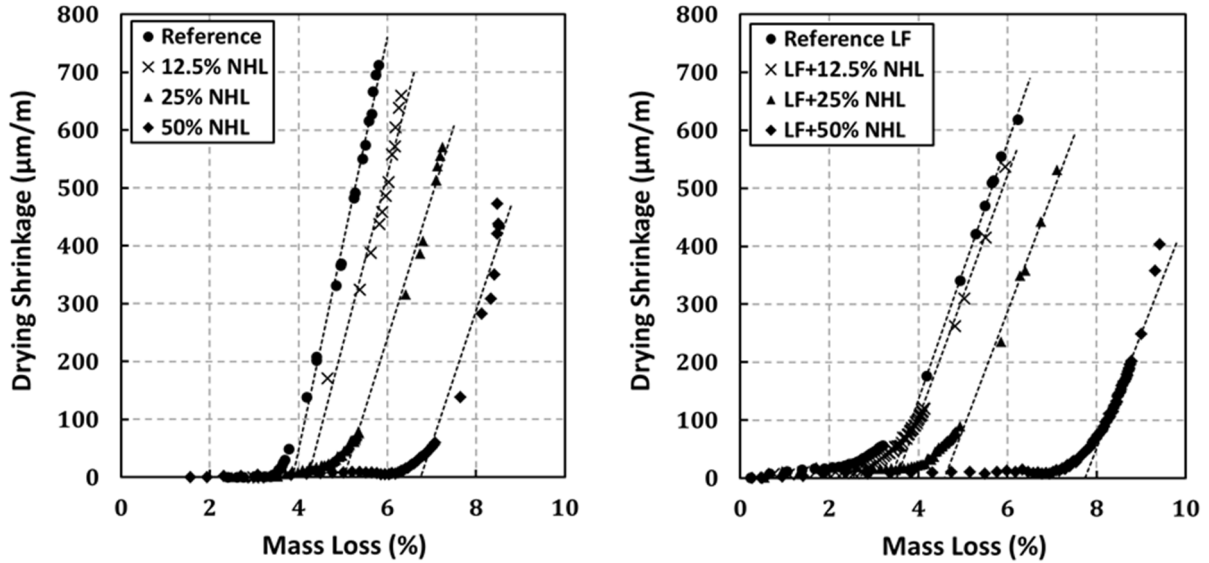


Figure 22 Ultimate drying shrinkage as function of the NHL content

Since drying shrinkage is due to water loss, mass loss and drying shrinkage versus mass loss relations can provide useful information to understand the trend observed for the drying shrinkage. Table V shows that, for increasing NHL substitution rates, the mass loss increased. Knowing that the hydration of the NHL is a rather slow process, and owing to the inert chemical nature of LF, the amount of free water in mixtures where NHL substitutes the cement is greater; thus apparent W/C ratio is higher. This is in line with the results of Bisonnette [73] which showed that the higher the W/C apparent ratio, the higher the weight loss. In Figure 23, drying shrinkage is plotted against weight loss for all the studied mixtures.

Table V Mass loss for studied mortars at 28d

	Without LF	With LF
Reference	5.8 %	6.0 %
12.5% NHL	6.5 %	6.0 %
25% NHL	7.5 %	7.1 %
50% NHL	8.5 %	9.3 %

**Figure 23 Drying shrinkage vs. Mass loss for studied mortars**

The drying shrinkage versus mass loss curves (Figure 23) allow defining two stages [74], [75]. The first stage occurs during the first days and is characterized by a high mass loss for a small variation in drying shrinkage. According to some authors, the evaporation of water close to the surface of the specimen is mainly responsible for the mass loss during the first days after the end of curing. Moreover, it also has been reported that evaporated water at early age mainly comes from large capillary pores [73]. According to Kelvin-Laplace (Equation 6) the capillary stress decreases with the pore radius, therefore, shrinkage decreases also with the pore radius. Thus, the capillary stress due to this initial water loss is not high enough to affect the shrinkage evolution. This first stage corresponding to initial mass loss was longer for mixtures with increasing rates of NHL due to the high free water content. Microcracking and structural effects also explain the first stage [76], as the shrinkage of the outer layer of the specimen is restrained by the central part. An increase in NHL proportion was actually found to lead to lower strength.

The second stage of drying shrinkage corresponds to a linear relationship between the deformation and the mass loss. It corresponds to the decrease of relative humidity and water content within the specimen. The slope of this curve is the parameter CF called hydrous compressibility factor [76], [77]. LF and NHL also affected the second phase leading to a decrease in the value of the parameter CF (Figure 24). The CF depends on the sizes of the pores in the mixture. The introduction of LF and NHL leads to the formation of larger pores, which results in lower decrease in capillary pressure and therefore lower drying shrinkage.

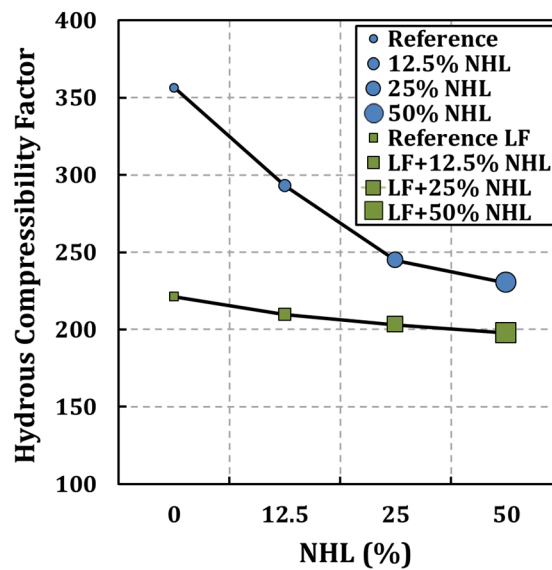


Figure 24 Hydrous compressibility factor as function of the NHL proportion

4. Conclusions

The study presented in this paper deals with the influence of natural hydraulic lime (NHL) on the behavior of cement-based materials. NHL substituted Portland cement at different proportions in mortars with and without limestone filler. A comprehensive experimental program has been designed to investigate the influence of NHL at early-age and long-term. From the results of the study several conclusions can be drawn.

- The incorporation of NHL resulted in lower packing density of the solid granular structure due to the lower packing density of NHL powder. This affected the rheological behavior, in terms of yield stress and apparent viscosity, but the homogeneity of the mortar mixtures was improved.
- The acceleration of the first stage of hydration with increasing NHL content did not systematically lead to earlier setting. Nucleation effect due to higher specific surface was actually in competition with dilution effect, especially when limestone filler was

added. At the highest NHL proportions, a higher hydration degree must be reached to induce a significant development of shear modulus.

- Several assumptions have been checked in order to understand the observed reduction in plastic shrinkage magnitude. This could be partly explained by the variations in setting time. A swelling stage was also observed on plastic shrinkage evolution for the highest NHL contents. As the chemical shrinkage evolution was not significantly influenced by NHL proportion, mechanical effects such as crystallization pressure could explain this behavior. Thermal analyses actually showed faster production of portlandite and ettringite during the acceleration period of hydration, while the stiffness of cement paste is relatively low.
- Compressive strength decreased with NHL proportion. However, an optimum was found at 12.5% with limestone filler. This corresponds to a physical effect on hydration and optimum specific surface for a given clinker content.
- NHL also mitigated long-term drying shrinkage. The first stage of drying was actually more pronounced, then the sensitivity of shrinkage strain to mass loss was also reduced, which corresponds to coarser porosity.

In this study natural hydraulic lime appeared as a promising way to optimize the mix-design of mortar mixtures in terms of workability, mechanical properties and delayed behavior. Cost-effectiveness and durability indicators should also be included to determine the optimum lime proportion.

5. References

- [1] A. Loukili, *Self-compacting concrete*. ISTE, 2011.
- [2] M. Lachemi, K. M. . Hossain, V. Lambros, P.-C. Nkinamubanzi, and N. Bouzoubaâ, “Self-consolidating concrete incorporating new viscosity modifying admixtures,” *Cement and Concrete Research*, vol. 34, no. 6, pp. 917–926, 2004.
- [3] Y. Sébaïbi, R. M. Dheilly, and M. Quéneudec, “A study of the viscosity of lime-cement paste: Influence of the physico-chemical characteristics of lime,” *Construction and Building Materials*, vol. 18, no. 9, pp. 653–660, 2004.
- [4] H. Güllü, “On the viscous behavior of cement mixtures with clay, sand, lime and bottom ash for jet grouting,” *Construction and Building Materials*, vol. 93, pp. 891–910, 2015.
- [5] E. R. Grist, K. A. Paine, A. Heath, J. Norman, and H. Pinder, “Structural and durability properties of hydraulic lime-pozzolan concretes,” *Cement and Concrete Composites*, vol. 62, pp. 212–223, 2015.
- [6] J. S. Pozo-Antonio, “Evolution of mechanical properties and drying shrinkage in lime-based and lime cement-based mortars with pure limestone aggregate,” *Construction and Building Materials*, vol. 77, pp. 472–478, 2015.
- [7] M. Arandigoyen and J. I. Alvarez, “Pore structure and mechanical properties of cement-lime mortars,” *Cement and Concrete Research*, vol. 37, no. 5, pp. 767–775, 2007.
- [8] M. Arandigoyen and J. I. Alvarez, “Blended pastes of cement and lime: Pore structure and capillary porosity,” *Applied Surface Science*, vol. 252, no. 23, pp. 8077–8085, 2006.
- [9] M. J. Mosquera, B. Silva, B. Prieto, and E. Ruiz-Herrera, “Addition of cement to lime-based mortars: Effect on pore structure and vapor transport,” *Cement and Concrete Research*, vol. 36, no. 9, pp. 1635–1642, Sep. 2006.
- [10] M. Arandigoyen, B. Bicer-Simsir, J. I. Alvarez, and D. A. Lange, “Variation of microstructure with carbonation in lime and blended pastes,” *Applied Surface Science*, vol. 252, no. 20, pp. 7562–7571, Aug. 2006.
- [11] P. K. Acharya, S. K. Patro, and N. C. Moharana, “Effect of Lime on Mechanical and Durability Properties of Blended Cement Based Concrete,” *Journal of The Institution of Engineers (India): Series A*, vol. 97, no. 2, pp. 71–79, 2016.
- [12] M. Fourmentin, P. Faure, S. Gauffinet, U. Peter, D. Lesueur, D. Daviller, G. Ovarlez, and P. Coussot, “Porous structure and mechanical strength of cement-lime pastes during setting,” *Cement and Concrete Research*, vol. 77, pp. 1–8, 2015.
- [13] M. Fourmentin, “Impact de la répartition et des transferts d’eau sur les propriétés des matériaux de construction à base de chaux formulées,” Thèse de doctorat, Université Paris-Est, 2015.
- [14] L. Nicoleau, “Accelerated growth of calcium silicate hydrates: Experiments and simulations,” *Cement and Concrete Research*, vol. 41, no. 12, pp. 1339–1348, 2011.
- [15] Ö. Cizer, K. Van Balen, and D. Van Gemert, “Competition between Hydration and Carbonation in Hydraulic Lime and Lime-Pozzolana Mortars,” *Advanced Materials Research*, vol. 133–134, pp. 241–246, Oct. 2010.
- [16] “Mineralogy of Raw Materials - Saint Astier® NHL.” [Online]. Available:

<https://limes.us/technical-info/mineralogy-chemistry-of-raw-materials/>. [Accessed: 15-Dec-2018].

- [17] P. F. G. Banfill, E. M. Szadurski, and A. M. Forster, “Deterioration of natural hydraulic lime mortars, II: Effects of chemically accelerated leaching on physical and mechanical properties of carbonated materials,” *Construction and Building Materials*, vol. 111, pp. 182–190, May 2016.
- [18] E. R. Grist, A. K. Paine, A. Heath, J. Norman, and H. Pinder, “The environmental credentials of hydraulic lime-pozzolan concretes,” *Journal of Cleaner Production*, vol. 93, pp. 26–37, Apr. 2015.
- [19] D. Zhang, J. Zhao, D. Wang, C. Xu, M. Zhai, and X. Ma, “Comparative study on the properties of three hydraulic lime mortar systems: Natural hydraulic lime mortar, cement-aerial lime-based mortar and slag-aerial lime-based mortar,” *Construction and Building Materials*, vol. 186, pp. 42–52, Oct. 2018.
- [20] P. Domone and C. Hsi-Wen, “Testing of binders for high performance concrete,” *Cement and Concrete Research*, vol. 27, no. 8, pp. 1141–1147, 1997.
- [21] H. Okamura, K. Maekawa, and K. Ozawa, *High performance concrete*. 1993.
- [22] R. Cortas, E. Rozière, S. Staquet, A. Hamami, A. Loukili, and M.-P. Delplancke-Ogletree, “Effect of the water saturation of aggregates on the shrinkage induced cracking risk of concrete at early age,” *Cement and Concrete Composites*, vol. 50, pp. 1–9, Jul. 2014.
- [23] A. Z. Bendimerad, E. Rozière, and A. Loukili, “Plastic shrinkage and cracking risk of recycled aggregates concrete,” *Construction and Building Materials*, vol. 121, pp. 733–745, 2016.
- [24] T. Lenormand, E. Rozière, A. Loukili, and S. Staquet, “Incorporation of treated municipal solid waste incineration electrostatic precipitator fly ash as partial replacement of Portland cement: Effect on early age behaviour and mechanical properties,” *Construction and Building Materials*, vol. 96, pp. 256–269, 2015.
- [25] M. Bouasker, P. Mounanga, P. Turcry, A. Loukili, and A. Khelidj, “Chemical shrinkage of cement pastes and mortars at very early age: Effect of limestone filler and granular inclusions,” *Cement and Concrete Composites*, vol. 30, no. 1, pp. 13–22, 2008.
- [26] H. W. Reinhardt and C. U. Grosse, “Continuous monitoring of setting and hardening of mortar and concrete,” *Construction and Building Materials*, vol. 18, no. 3, pp. 145–154, Apr. 2004.
- [27] M. Krüger, R. Bregar, G. A. David, and J. Juhart, “Non-destructive evaluation of eco-friendly cementitious materials by ultrasound,” in *Proceedings of the International RILEM Conference : Materials, Systems and Structures in Civil Engineering*, 2016, pp. 503–512.
- [28] “Partie 1: Détermination des résistances mécaniques. NF EN 196-1,” in *Méthodes d’essais des ciments*, 2016.
- [29] E. Rozière, S. Granger, P. Turcry, and A. Loukili, “Influence of paste volume on shrinkage cracking and fracture properties of self-compacting concrete,” *Cement and Concrete Composites*, vol. 29, no. 8, pp. 626–636, 2007.
- [30] D. P. Bentz, C. F. Ferraris, M. A. Galler, A. S. Hansen, and J. M. Guynn, “Influence of particle size distributions on yield stress and viscosity of cement–fly ash pastes,” *Cement and Concrete Research*, vol. 42, no. 2, pp. 404–409, Feb. 2012.

- [31] O. Esping, "Effect of limestone filler BET(H₂O)-area on the fresh and hardened properties of self-compacting concrete," *Cement and Concrete Research*, vol. 38, no. 7, pp. 938–944, 2008.
- [32] F. Michel, J. Pierard, L. Courard, and V. Pollet, "Influence of physic-chemical characteristics of limestone fillers on fresh and hardened mortar performances," in *5th International RILEM Symposium on Self-Compacting Concrete, Proceedings PRO 54*, 2007, pp. 205–210.
- [33] C. F. Ferraris, K. H. Obla, and R. Hill, "The influence of mineral admixtures on the rheology of cement paste and concrete," *Cement and Concrete Research*, vol. 31, no. 2, pp. 245–255, 2001.
- [34] N. Shanahan, V. Tran, A. Williams, and A. Zayed, "Effect of SCM combinations on paste rheology and its relationship to particle characteristics of the mixture," *Construction and Building Materials*, vol. 123, pp. 745–753, Oct. 2016.
- [35] N. Roussel, "Correlation between Yield Stress and Slump: Comparison between Numerical Simulations and Concrete Rheometers Results," *Materials and Structures*, vol. 39, no. 4, pp. 501–509, Aug. 2007.
- [36] T. Sedran and F. De Larrard, "Optimization of self-compacting concrete thanks to packing model," in *1st International RILEM Symposium on Self-Compacting Concrete*, 1999, pp. 321–332.
- [37] F. De Larrard and T. Sedran, "Mixture-proportioning of high-performance concrete," *Cement and Concrete Research*, vol. 32, pp. 1699–1704, 2002.
- [38] E. Berodier and K. Scrivener, "Understanding the Filler Effect on the Nucleation and Growth of C-S-H," *Journal of the American Ceramic Society*, vol. 97, no. 12, pp. 3764–3773, Dec. 2014.
- [39] L. Stefan, F. Benboudjema, J. M. Torrenti, and B. Bissonnette, "Prediction of elastic properties of cement pastes at early ages," *Computational Materials Science*, vol. 47, no. 3, pp. 775–784, 2010.
- [40] E. H. Kadri, S. Aggoun, G. De Schutter, and K. Ezziane, "Combined effect of chemical nature and fineness of mineral powders on Portland cement hydration," *Materials and Structures*, vol. 43, no. 5, pp. 665–673, Jun. 2010.
- [41] A. Schöler, B. Lothenbach, F. Winnefeld, M. Ben Haha, M. Zajac, and H.-M. Ludwig, "Early hydration of SCM-blended Portland cements: A pore solution and isothermal calorimetry study," *Cement and Concrete Research*, vol. 93, pp. 71–82, Mar. 2017.
- [42] W. Lerch, "The influence of gypsum on the hydration and properties of Portland cement pastes," *American Society for Testing Materials*, vol. 46, pp. 1252–1297, 1946.
- [43] C. Hesse, F. Goetz-Neunhoeffler, and J. Neubauer, "A new approach in quantitative in-situ XRD of cement pastes: Correlation of heat flow curves with early hydration reactions," *Cement and Concrete Research*, vol. 41, no. 1, pp. 123–128, Jan. 2011.
- [44] D. Jansen, F. Goetz-Neunhoeffler, B. Lothenbach, and J. Neubauer, "The early hydration of Ordinary Portland Cement (OPC): An approach comparing measured heat flow with calculated heat flow from QXRD," *Cement and Concrete Research*, vol. 42, no. 1, pp. 134–138, Jan. 2012.
- [45] A.-M. Poppe and G. De Schutter, "Cement hydration in the presence of high filler contents," *Cement and Concrete Research*, vol. 35, no. 12, pp. 2290–2299, 2005.

- [46] S. Garrault and A. Nonat, "Hydrated layer formation on tricalcium and dicalcium silicate surfaces: Experimental study and numerical simulations," vol. 17, pp. 8131–8138, 2001.
- [47] A. Darquennes, M. I. A. Khokhara, E. Rozière, A. Loukili, F. Grondin, and S. Staquet, "Early age deformations of concrete with high content of mineral additions," *Construction and Building Materials*, vol. 25, no. 4, pp. 1836–1847, Apr. 2011.
- [48] H. Le Chatelier, "Sur le changement de volume qui accompagne le durcissement des ciments," *Bulletin de la Société de l'encouragement pour l'industrie nationale*, vol. 5, no. 5, pp. 54–57, 1900.
- [49] G. Ye, X. Liu, G. De Schutter, A.-M. Poppe, and L. Taerwe, "Influence of limestone powder used as filler in SCC on hydration and microstructure of cement pastes," *Cement and Concrete Composites*, vol. 29, no. 2, pp. 94–102, 2007.
- [50] M. Wyrzykowski, P. Trtik, B. Münch, J. Weiss, P. Vontobel, and P. Lura, "Plastic shrinkage of mortars with shrinkage reducing admixture and lightweight aggregates studied by neutron tomography," *Cement and Concrete Research*, vol. 73, pp. 238–245, 2015.
- [51] J.-C. Souche, A. Z. Bendimerad, E. Roziere, M. Salgues, P. Devillers, E. Garcia-Diaz, and A. Loukili, "Early age behaviour of recycled concrete aggregates under normal and severe drying conditions," *Journal of Building Engineering*, vol. 13, pp. 244–253, Sep. 2017.
- [52] W. J. Weiss, P. Lura, F. Rajabipour, and G. Sant, "Performance of Shrinkage-Reducing Admixtures at Different Humidities and at Early Ages," *ACI Materials Journal*, vol. 105, no. 5, 2008.
- [53] D. P. Bentz, M. R. Geiker, and K. K. Hansen, "Shrinkage-reducing admixtures and early-age desiccation in cement pastes and mortars," *Cement and Concrete Research*, vol. 31, no. 7, pp. 1075–1085, 2001.
- [54] D. P. Bentz, "Curing with shrinkage-reducing admixtures: beyond drying shrinkage reduction," *Concrete International*, vol. 27, pp. 51–60, 2005.
- [55] J. Saliba, E. Rozière, F. Grondin, and A. Loukili, "Influence of shrinkage-reducing admixtures on plastic and long-term shrinkage," *Cement and Concrete Composites*, vol. 33, no. 2, pp. 209–217, 2011.
- [56] D. Cusson, "Effect of blended cements on effectiveness of internal curing of HPC," *ACI Special Publication*, vol. 256, pp. 105–120, 2008.
- [57] E. Roziere, R. Cortas, and A. Loukili, "Tensile behaviour of early age concrete: New methods of investigation," *Cement and Concrete Composites*, vol. 55, pp. 153–161, 2015.
- [58] M. D. Cohen, J. Olek, and W. L. Dolch, "Mechanism of plastic shrinkage cracking in portland cement and portland cement-silica fume paste and mortar," *Cement and Concrete Research*, vol. 20, no. 1, pp. 103–119, 1990.
- [59] P. Lura, B. Pease, G. B. Mazzotta, and W. J. Weiss, "Influence of shrinkage-reducing admixtures on development of plastic shrinkage cracks," *ACI Materials Journal*, vol. 104, pp. 187–194, 2007.
- [60] F. H. Wittmann, "On the action of capillary pressure in fresh concrete," *Cement and Concrete Research*, vol. 6, no. 1, pp. 49–56, 1976.
- [61] T. Hammer, Ø. Bjøntegaard, and E. Sellevold, "Measurement methods for testing of early age

- autogenous strain,” in *Bentur A (ed) Early age cracking in cementitious systems. RILEM TC 181-EAS Committee, RILEM, Cachan*, pp. 234–245.
- [62] G. Sant, B. Lothenbach, P. Juilland, G. Le Saout, J. Weiss, and K. Scrivener, “The origin of early age expansions induced in cementitious materials containing shrinkage reducing admixtures,” *Cement and Concrete Research*, vol. 41, no. 3, pp. 218–229, 2011.
- [63] I. Odler, “Expansive cements,” in *Special Inorganic Cements (Modern Concrete Technology)*, 1st ed., CRC Press, 2000, pp. 316–335.
- [64] W. Müllauer, R. E. Beddoe, and D. Heinz, “Sulfate attack expansion mechanisms,” *Cement and Concrete Research*, vol. 52, pp. 208–215, Oct. 2013.
- [65] G. W. Scherer, “Crystallization in pores,” *Cement and Concrete Research*, vol. 29, no. 8, pp. 1347–1358, Aug. 1999.
- [66] G. W. Scherer, “Stress from crystallization of salt,” *Cement and Concrete Research*, vol. 34, no. 9, pp. 1613–1624, Sep. 2004.
- [67] D. Min and T. Mingshu, “Formation and expansion of ettringite crystals,” *Cement and Concrete Research*, vol. 24, pp. 119–126, 1994.
- [68] Y. Tezuka, J. G. Djanikan, H. Uchikawa, and S. Uchida, “Hydration characteristics and properties of mixtures of cement and high content of calcium,” in *Symp. on Chemistry of Cement*, 1986, pp. 323–329.
- [69] C. Vernet and G. Cadoret, “Suivi en continu de l’évolution chimique et mécanique des BHP pendant les premiers jours (in French), Les Bétons à Hautes Performances – Caractérisation, durabilité applications,” *Presses de l’Ecole Nationale des Ponts et Chaussées, Paris, France*, 1992.
- [70] O. Çizer, *Competition between carbonation and hydration on the hardening of calcium hydroxide and calcium silicate binders*. 2009.
- [71] M. Cyr, P. Lawrence, and E. Ringot, “Efficiency of mineral admixtures in mortars: Quantification of the physical and chemical effects of fine admixtures in relation with compressive strength,” *Cement and Concrete Research*, vol. 36, no. 2, pp. 264–277, 2006.
- [72] C. H. Torben and A. H. Mattock, “Influence of Size and Shape of Member on the Shrinkage and Creep of Concrete,” *ACI Journal Proceedings*, vol. 63, no. 2, 1966.
- [73] B. Bissonnette, P. Pierre, and M. Pigeon, “Influence of key parameters on drying shrinkage of cementitious materials,” *Cement and Concrete Research*, vol. 29, no. 10, pp. 1655–1662, 1999.
- [74] H. Samouh, A. Soive, E. Rozière, and A. Loukili, “Experimental and numerical study of size effect on long-term drying behavior of concrete: influence of drying depth,” *Materials and Structures*, vol. 49, no. 10, pp. 4029–4048, Oct. 2016.
- [75] A. Darquennes, E. Rozière, M. I. A. Khokhar, P. Turcry, A. Loukili, and F. Grondin, “Long-term deformations and cracking risk of concrete with high content of mineral additions,” *Materials and Structures*, vol. 45, no. 11, pp. 1705–1716, Nov. 2012.
- [76] F. Benboudjema, F. Meftah, and J. M. Torrenti, “Interaction between drying, shrinkage, creep and cracking phenomena in concrete,” *Engineering Structures*, vol. 27, no. 2, pp. 239–250, 2005.

- [77] L. Granger, J.-M. Torrenti, and P. Acker, "Thoughts about drying shrinkage: Experimental results and quantification of structural drying creep," *Materials and Structures*, vol. 30, no. 10, pp. 588–598, Dec. 1997.